Sheffield Hallam University

Simulation study of the Gilbert Damping in Ni80Fe20/Nd Bilayers: comparison with experiments.

CAO, LuLu <http://orcid.org/0009-0005-7572-5780>, RUTA, Sergiu <http://orcid.org/0000-0001-8665-6817>, KHAMTAWI, Rungtawan, CHUREEMART, Phanwadee <http://orcid.org/0000-0002-1199-7809>, ZHAI, Ya <http://orcid.org/0000-0002-9006-9575>, EVANS, Richard FL <http://orcid.org/0000-0002-2378-8203> and CHANTRELL, Roy W

Citation:

Copyright and re-use policy

Simulation study of the Gilbert damping in Ni$_{80}$Fe$_{20}$/Nd bilayers: comparison with experiments

To cite this article: Lulu Cao *et al* 2024 *J. Phys.: Condens. Matter* **36** 305901

View the [article online](#) for updates and enhancements.

Simulation study of the Gilbert damping in Ni₈₀Fe₂₀/Nd bilayers: comparison with experiments

Lulu Cao[1,2] , **Sergiu Ruta**[3] , **Rungtawan Khamtawi**[4] , **Phanwadee Chureemart**[4] ,
Ya Zhai[1,*] , **Richard F L Evans**[2,*] and **Roy W Chantrell**[2,*]

[1] Key Laboratory of Quantum Materials and Devices of Ministry of Education, School of Physics,
Southeast University, Nanjing 211189, People's Republic of China
[2] Department of Physics, Engineering and Technology, University of York, York YO10 5DD, United
Kingdom
[3] Sheffield Hallam University-Collegiate Campus, Sheffield S10 2BP, United Kingdom
[4] Department of Physics, Mahasarakham University, Mahasarakham 44150, Thailand

E-mail: yazhai@seu.edu.cn, Richard.evans@york.ac.uk and roy.chantrell@york.ac.uk

CrossMark

Abstract
We present an experimental and computational investigation the Neodymium thickness
dependence of the effective damping constant (α_{eff}) in $Ni_{80}Fe_{20}$/Neodymium (Py/Nd) bilayers.
The computational results show that the magnetic damping is strongly dependent on the
thickness of Nd, which is in agreement with experimental data. Self consistent solutions of the
spin accumulation model and the local magnetisation were used in the simulations. It was not
possible to obtain agreement with experiment under the assumption of an enhanced damping in
a single Py monolayer. Instead, it was found that the enhanced damping due to spin pumping
needed to be spread across two monolayers of Py. This is suggested to arise from interface
mixing. Subsequently, the temperature dependence of the effective damping was investigated. It
is found that, with increasing temperature, the influence of thermally-induced spin fluctuations
on magnetic damping becomes stronger with increasing Nd thickness.

Supplementary material for this article is available online

Keywords: spin accumulation model, spin pumping, atomistic spin model

1. Introduction

Recently, spintronic devices based on magnetic dynamics, such as magnetic random-access memory, spin valve (SV), magnetic tunnel junction and so on, have attracted extensive attention [1–3]. The Gilbert damping parameter α as a characteristic of magnetisation dynamics is a major focus of research due to its effect on the speed of the magnetisation reversal. As a typical transition magnetic (TM) alloy, Permalloy has a high saturation magnetisation and permeability, low anisotropy and coercivity. Permalloy ($Ni_{80}Fe_{20}$, Py) has a small magnetic damping, which is due to the fact that the crystal field will quench the most of orbital momentum, resulting in a small spin orbit coupling. So, it is necessary to increase the magnetic damping to increase the magnetic response. There are mainly two methods to regulate magnetic

damping, i.e. doping and magnetic heterostructures [4–8]. Rare earth elements (RE) have a large orbital moment, which could increase the spin-orbit coupling and magnetic damping in RE-TM systems. In 2002, Tserkovnyak *et al* [9, 10] proposed the spin pumping effect: in ferromagnetic/nonmagnetic (FM/NM) bilayer, the magnetisation precession acts as spin pump which transfers angular momentum from the FM layer into the NM layer which is then dissipated in the NM layer. This dissipation increases the relaxation of the magnetic moment precession in the FM layer and leads to an increase of magnetic damping. The enhanced magnetic damping is represented by the scattering matrix of the FM layer.

In this paper, we present experimental and theoretical investigations of the Nd thickness dependence of the effective damping constant (α_{eff}) in $Ni_{80}Fe_{20}$/Neodymium (Py/Nd) bilayers. In experiments, the magnetic damping can be easily obtained by vector network analyser ferromagnetic resonance (VNA-FMR) in comparison with Brillouin light scattering and time-resolved magneto-optical Kerr effect. VNA-FMR is a standard and widely used tool to measure the magnetic damping by analysing the relationship between frequency and linewidth of the resonance spectrum. The FMR linewidth has two contributions: one is the intrinsic damping coming from the Py film; the other arises from a spin pumping effect which pumps a spin current from the Py layer to Nd the layer.

In experiments, there are a number of reasons for enhanced magnetic damping, including the contribution of enhanced spin orbit coupling at the interface, and dispersions in material properties which results in inhomogeneous line broadening. The important mechanism of the spin pumping effect is rarely considered, whereas spin pumping, and especially its dependence on the thickness of a non-magnetic layer, could be considered an interesting method of damping enhancement and control. So, we use the spin accumulation methodology to simulate the bilayer structures based on the drift-diffusion formalism of Zhang *et al* [11]. Based on previous works, we introduce the bulk and interface magnetic damping to investigate the thickness dependence in Py/Nd bilayer films [12–14]. So, the appropriate values of the bulk and interface damping are essential for a theoretical calculation for comparison with the experimental data. Py itself has a very low anisotropy. So, we set the same anisotropy energy values for bulk Py layers. Then the high interface magnetic damping values in interface Py comes from the spin pumping effect [15]. The simulation of our bilayer structure is modelled by using the stochastic Landau–Lifshitz–Gilbert (LLG) equation at the atomistic level and the VAMPIRE software package [16, 17]. Meanwhile, with increasing temperature, the other scattering mechanism, i.e. thermal-spin fluctuations leading to spin-wave excitations are naturally taken into account in the atomistic approach. In order to study the influence of thermal-spin fluctuations in the Py/Nd bilayer, the temperature variation of the effective Gilbert damping is also studied.

2. Simulation

2.1. The spin accumulation model

The concept of spin injection into a normal metal leading to a spin accumulation of electron polarisation was put forward by Aronov [18] and has been enriched and developed by many research groups [11, 19, 20]. This spin accumulation decays on a length scale characterised by the spin difusion length (sdl). According to the formula derived by Zhang *et al* [11], in a magnetic heterostructure the equation of motion for the spin accumulation is,

$$\frac{\text{d}\boldsymbol{m}}{\text{d}t} + (J_{sd}/\hbar)\,\mathbf{m} \times \mathbf{M}_d = -\frac{\mathbf{m}}{\tau_{\text{sf}}}, \tag{1}$$

where $\mathbf{m}$ is the spin accumulation, $\mathbf{M}_d$ is the unit vector for the local magnetisation of the FM layer, J_{sd} is the exchange energy between the electron spin and the local magnetisation, $\hbar$ is the reduced Planck constant, τ_{sf} is the spin–flip relaxation time of the conduction electrons. In order to obtain a stationary solution for spin accumulation m, the spin-flip relaxation time of the conduction electrons τ_{sf} should be shorter than the timescale of the magnetisation changes.

The equation of motion for the local magnetisation is

$$\frac{\text{d}\mathbf{M}_d}{\text{d}t} = -\gamma\mathbf{M}_d \times (\mathbf{H}_{\text{eff}} + J_{sd}\mathbf{m}) + \alpha\mathbf{M}_d \times \frac{\text{d}\mathbf{M}_d}{\text{d}t} \tag{2}$$

where γ is the gyromagnetic ratio, α is the magnetic damping constant, $\mathbf{H}_{\text{eff}}$ is the effective field, which includes the external field, exchange, magnetostatic and crystalline anisotropy field. $J_{sd}\mathbf{m}$ is the field arising from the conduction electron/magnetic spin exchange.

In general, the magnetisation direction and the spin accumulation are not collinear. The spin accumulation be separated into two components: longitudinal mode (parallel to the local magnetisation direction) and transverse mode (perpendicular to the local magnetisation direction). So, the two components spin accumulation can be expressed as

$$\frac{\partial^2 \mathbf{m}_{\parallel}}{\partial x^2} - \frac{\partial^2 \mathbf{m}_{\parallel}}{\lambda_{\text{sdl}}^2} = 0 \tag{3}$$

and

$$\frac{\partial^2 \mathbf{m}_{\perp}}{\partial x^2} - \frac{\partial^2 \mathbf{m}_{\perp}}{\lambda_{\text{sf}}^2} - \frac{\mathbf{m}_{\perp} \times \mathbf{M}_d}{\lambda_J^2} = 0, \tag{4}$$

where $\lambda_{\text{sf}} = \sqrt{2D_0\tau_{sf}}$, $\lambda_J = \sqrt{\frac{2\hbar D_0}{J_{sd}}}$, D_0 is the diffusion constant.

In the general case the solution for the spin accumulation can be obtained using a transfer matrix method [19]. However, according to Heide *et al* [21] only the longitudinal accumulation exists for a single FM layer, while the transverse accumulation is required for a 'SV' structure. That means we can simply consider the longitudinal component of spin accumulation in our structure. The current is perpendicular to the plane
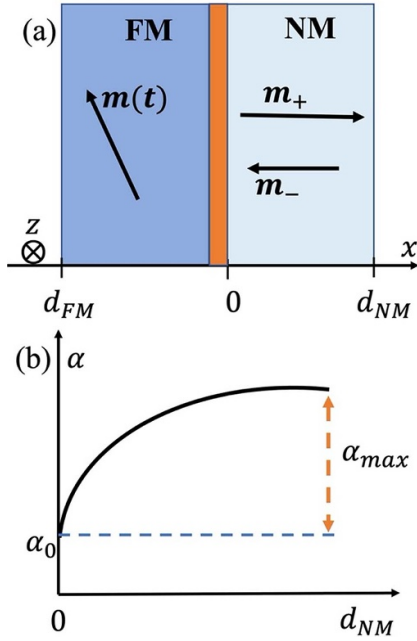
Figure 1. (a) Schematic view of FM/NM bilayer. The dark blue and the orange represent the bulk FM layer and interface FM layer, respectively. The light blue represents the NM layer. Precession of the magnetisation direction $m(t)$ of the FM pumps a spin current into the NM layer. $\mathbf{m}_+$ and $\mathbf{m}_-$ are pumped and reflected spin accumulation in NM layer, respectively. (b) The curve of effective Gilbert damping ($\alpha_{\mathrm{eff}} = \alpha_0 + \alpha_{\mathrm{max}}$) comes from spin pumping theory. α_0 is the intrinsic damping. α_{max} is the maximum Gilbert damping increase.

of the films. As shown in figure 1(a), the pumped spin accumulation whose magnetisation direction is at the positive z direction is given by the following equation,

$$\mathbf{m}_+ (x) = \mathbf{m}_0 e^{\frac{-x}{\lambda_{\mathrm{sdl}}}} \tag{5}$$

where $\mathbf{m}_0 = \frac{\lambda_{\mathrm{sdl}}}{4D_0} j_{mx}(0)$ is the pre-exponential factor for the pumped spin accumulation. $j_{mx}(0)$ is the spin current transmitted from the FM to the NM, given by [9, 10]

$$j_{mx}(0) = \frac{\hbar g_r^{\uparrow\downarrow}}{4\pi M^2} \left(\mathbf{M} \times \frac{\partial \mathbf{M}}{\partial t} \right), \tag{6}$$

with $g_r^{\uparrow\downarrow}$ the spin mixing conductance. The reflected spin accumulation at the vacuum boundary of the non-magnet is given by

$$\mathbf{m}_- (x) = \mathbf{A} e^{\frac{(x - d_{\mathrm{NM}})}{\lambda_{\mathrm{sdl}}}}, \tag{7}$$

where A is the pre-exponential factor for the reflected spin accumulation, d_{NM} is the thickness of NM layer. So, the spin accumulation in the steady state as follows,

$$\mathbf{m} = \mathbf{m}_+ (x) + \mathbf{m}_- (x). \tag{8}$$

Then the spin current density in x direction calculated from the spin accumulation is given by

$$j_m (x) = -\frac{\mathrm{d}}{\mathrm{d}x} \left[\mathbf{m}_+ (x) + \mathbf{m}_- (x) \right] = \frac{\mathbf{m}_0}{\lambda_{\mathrm{sdl}}} e^{\frac{-x}{\lambda_{\mathrm{sdl}}}} - \frac{\mathbf{A}}{\lambda_{\mathrm{sdl}}} e^{\frac{(x - d_{\mathrm{NM}})}{\lambda_{\mathrm{sdl}}}}. \tag{9}$$

At the right vacuum boundary of the NM layer, we set the current to zero, $j_m (d) = 0$,

$$\frac{\mathbf{m}_0}{\lambda_{\mathrm{sdl}}} e^{\frac{-x}{\lambda_{\mathrm{sdl}}}} - \frac{\mathbf{A}}{\lambda_{\mathrm{sdl}}} e^{\frac{(x - d_{\mathrm{NM}})}{\lambda_{\mathrm{sdl}}}}. \tag{10}$$

Then we obtain the pre-exponential factor: $\mathbf{A} = \frac{\mathbf{m}_0}{\lambda_{\mathrm{sdl}}} e^{\frac{d_{\mathrm{NM}}}{\lambda_{\mathrm{sdl}}}}$. Hence,

$$j_m (x) = \frac{\mathbf{m}_0}{\lambda_{\mathrm{sdl}}} \left(e^{\frac{-x}{\lambda_{\mathrm{sdl}}}} - e^{\frac{(x - d_{\mathrm{NM}})}{\lambda_{\mathrm{sdl}}}} \right) \tag{11}$$

and at the FM/NM interface ($x = 0$), the net spin current is given by,

$$j_m^{\mathrm{int}} = \frac{j_{mx}(0)}{\lambda_{\mathrm{sdl}}} \left(1 - e^{\frac{-2d_{\mathrm{NM}}}{\lambda_{\mathrm{sdl}}}} \right). \tag{12}$$

According to spin pumping theory, the effective magnetic damping including the intrinsic damping of FM layer and the net spin current at the FM/NM interface. So, the interface damping of the FM layer is given by,

$$\alpha_{\mathrm{int}} = \alpha_{\mathrm{max}} \left(1 - e^{\frac{-2d_{\mathrm{NM}}}{\lambda_{\mathrm{sdl}}}} \right) \tag{13}$$

where α_{max} is the enhanced magnetic damping and is proportional to the interface spin-mixing conductance $G^{\uparrow\downarrow}$. Therefore, the interface damping increases to an asymptotic value with the thickness of NM as shown in figure 1(b). For larger thicknesses, the increase in damping took the interfacial value to supercritical values ($\alpha > 1$) which led to fictitious dynamics. Therefore, we distribute the interfacial damping among the two Py layers nearest to the interface as the spin-pumping current is an interface effect. This is an interesting observation which suggests some intermixing at the Py/Nd interface.

The magnetization dynamics was simulated using an atomistic model via integration of the LLG equation.

$$\frac{\partial \mathbf{S}}{\partial t} = -\frac{\gamma}{(1 + \alpha^2)} (\mathbf{S} \times \mathbf{B_{eff}}) - \frac{\gamma\alpha}{(1 + \alpha^2)} [\mathbf{S} \times (\mathbf{S} \times \mathbf{B_{eff}})]. \tag{14}$$

The effective field, $\mathbf{B}_{\mathrm{eff},i} = -\frac{1}{\mu_s} \frac{\partial \mathcal{H}}{\partial \mathbf{S}_i}$, can be calculated from the Heisenberg spin Hamiltonian describing the energy contributions of the magnetic system given by:

$$\mathcal{H} = -\sum_{i<j} J_{ij} \mathbf{S}_i \cdot \mathbf{S}_j - k_{\mathrm{u}} \sum_i (\mathbf{S}_i \cdot \mathbf{e})^2 - \sum_i \mu_s^i \mathbf{S}_i \cdot \mathbf{B}_{\mathrm{app}}, \tag{15}$$

where $\mathbf{S}_{ij}$ is the unit vector of spin on site (i, j), J_{ij} is the nearest neighbour exchange integral between spin sites i and j, k_{u} is

the uniaxial anisotropy constant, γ is the absolute value of gyromagnetic ratio, α is the damping constant of the material. The terms on the right-hand-side of equation (15) represent the contribution of the exchange energy, the anisotropy energy and the Zeeman energy, respectively. Atomistic calculations were carried out using the VAMPIRE package [17].

3. Results

3.1. The thickness dependence of effective damping

The Py (6 nm)/Nd (t nm) structure is built as a bulk face-centred-cubic crystal with lattice constant of 3.54 Å. The structure, with dimensions of $20 \times 20 \times (6 + t)$ nm^3, is considered as a trilayer system consisting of a 2-monolayers-Py (interface-Py) in contact with the bulk-Py and varying thickness of Nd layer as shown in figure 2(a). To verify the correctness of the magnetic parameters of the trilayer structure and the method, the thickness dependence of the effective damping at 300 K is calculated first and then compared with the experimental work (as shown in supplementary S1). The magnetic parameters of the trilayer are shown in table 1. Here we introduce an anisotropy and exchange energy [22–24]. The interface magnetic damping of the Py in trilayer system obtained from the experimental data using equation (13) in this simulation are shown in figure 2(b), and the interface magnetic damping of the Py are shown in supplementary S2. Nd is a light RE material with antiferromagnetic transition temperature of 19.3 K [25, 26]. It shows that Nd exhibits paramagnetism at room temperature.

In simulations, the external field (10 T) is applied along the z direction. The magnetization is initially oriented in the yz plane at an angle of 30 deg to the applied field (z-direction) from where it undergoes damped precession into the field direction. A typical time evolution of the x and z component of the magnetisation precession obtained from the atomistic model are shown in figure 3(a). For different thickness of Nd, the precession frequency of the Py layer and the relaxation time are extracted, as the net magnetisation of the system evolves back to equilibrium state, using the following equation,

$$M(t) = A\exp\left(-\frac{t}{\tau}\right)\sin\left(2\pi ft\right) \qquad (16)$$

where A, f, τ are the amplitude of the magnetisation, the precession frequency and the relaxation time, respectively. The effective magnetic damping (α_{eff}) can be determined from the damped precession parameters as $\alpha_{\text{eff}} = \frac{1}{2\pi f\tau}$. Using this approach, the precession frequency and damping were calculated as a function of the Nd layer thickness.

By comparing the experimental data with the simulations, for zero Nd thickness, as shown in figure 3(b), the damping value is equal to the input Py value, $\alpha_{\text{eff}} = 0.0099$. Further, this value is consistent with our experimental result and other
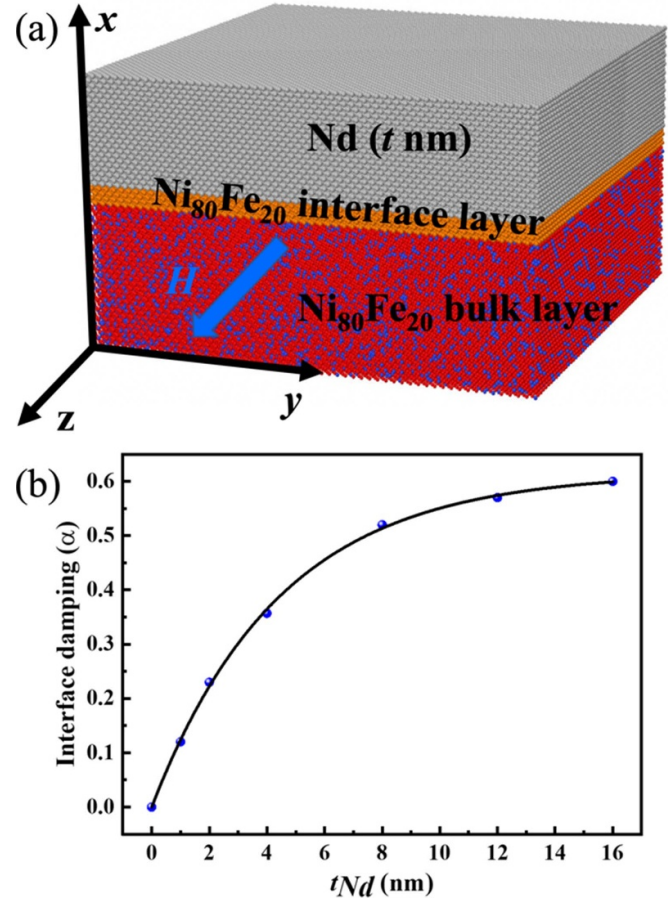

Figure 2. (a) Schematic view of the simulated (6 nm) Py/(t nm) Nd bilayer. The structure dimensions are $20 \times 20 \times (6 + t)$ nm^3, where the underlayer (red represent Ni atoms and blue represent the Fe atoms) and the orange inserted layer represents the bulk and interface Py layer, respectively. The grey square represents the Nd layer. (b) The variation of the interface damping and the thickness of Nd. The lines are a guide to the eye.

Table 1. Model parameters used in the simulation.

Parameter	Value	Unit
Atomic spin current μ_{Ni}	0.606	μ_B
Atomic spin current μ_{Fe}	2.22	μ_B
$J_{\text{Ni–Ni}}$	2.757×10^{-21}	J/link
$J_{\text{Fe–Fe}}$	7.05×10^{-21}	J/link
$J_{\text{Ni–Fe}}$	4.95×10^{-21}	J/link
Anisotropy energy k_{Ni}	5.47×10^{-26}	J/atom
Anisotropy energy k_{Fe}	5.65×10^{-25}	J/atom
Bulk damping of Ni and Fe	0.01	—

groups [13, 27]. This result shows that the calculated damping value of the bulk-Py is reasonable. By varying the interface magnetic damping according to the thickness of Nd, we also obtained the effective damping values as a function of Nd thickness. Comparison with the experimental data gives good agreement as shown in figure 3(b) indicating the validity of the atomistic model with spin accumulation and the input parameters.
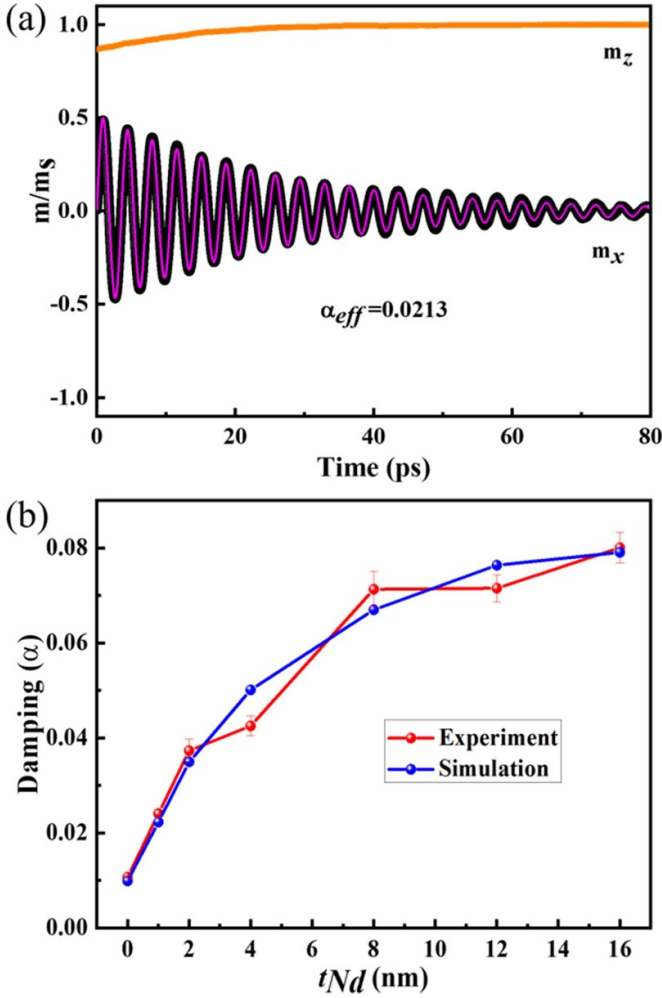
Figure 3. (a) The time evolution of the magnetisation trace of the Py (6 nm)/Nd (1 nm) structure at 300 K after an initial magnetisation angle of $30°$ in the *y*–*z* plane back to equilibrium state. The circle represents the simulated magnetisation precession while the lines are the fitting curve using equation (16). (b) The variation of the Gilbert damping and thickness of Nd. The lines are guided to the eye.

3.2. The temperature dependence of the effective magnetic damping

Further, we investigated the thickness dependence of the effective magnetic damping as a function of the temperature. In order to obtain statistically accurate results, we performed 10 different integrator-random-seeds for each parameter set, and then took the average and variance to obtained the mean magnetic damping.

Following [16], the thermal-spin fluctuations are introduced via a random field calculated as,

$$B_{th}(t) = \Gamma(t)\sqrt{\frac{2\alpha k_B T}{\gamma \mu_s \Delta t}} \tag{17}$$

where $\Gamma(t)$ is Gaussian distribution, T is the temperature in kelvin. k_B is the Boltzmann constant, μ_s is the atomic magnetic
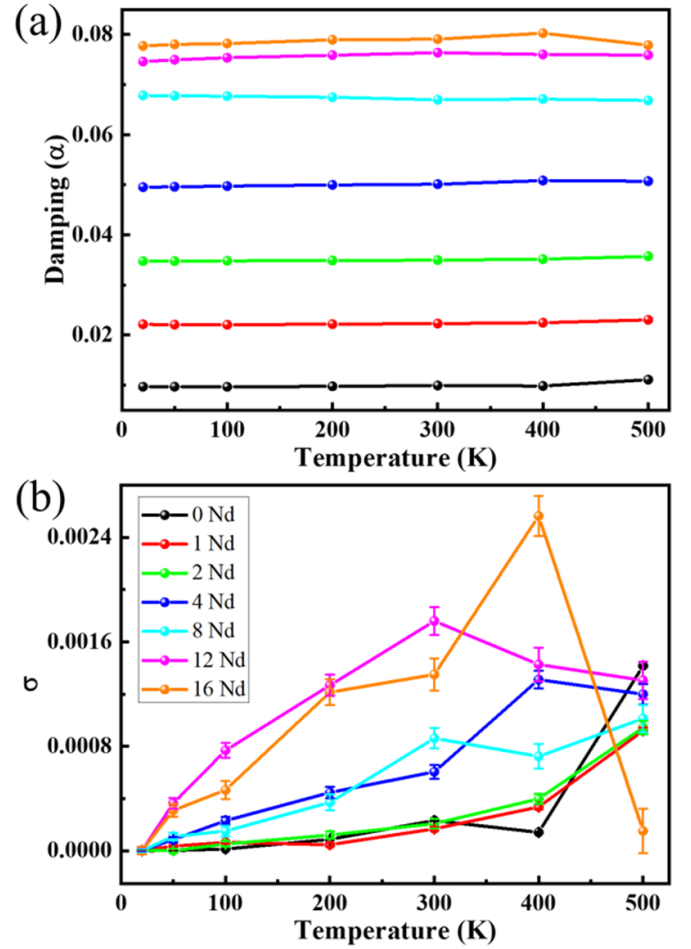

Figure 4. (a) is the mean magnetic damping of Py (6 nm)/Nd (t nm) bilayers with different temperature and Nd thickness. The lines are guided to lines. (b) The temperature dependence of the standard deviation (σ) of the distribution of the simulated magnetic damping constants as a function of the film thickness. The lines are guided to the eye.

moment, $\frac{2\alpha k_B T}{\gamma \mu_s}$ is the strength of the thermal-spin fluctuations. The thermal-spin fluctuation field is recalculated at each timestep and included in the effective local field.

Figure 4(a) shows the temperature dependence of the magnetic damping at different Nd thickness. From the data it can be seen that the temperature has a weak influence on the mean effective magnetic damping as also noted by Sampan-a-pai *et al* [22] for a single layer of CoFeB well below T_c. Interestingly, similarly to [22] we also observe statistical scatter in the calculated damping, albeit at a lower level. The standard deviation increases with Nd thickness, as shown in figure 4(b), suggesting that the effect is proportional to the damping. This is likely due to statistical variations arising from the finite size of the sample as in [22] and will decrease with increasing system size. To further investigate the influence of the temperature on effective magnetic damping, the magnetic dynamic relaxation process at different temperatures are shown in figure 5 for a Py (6 nm)/Nd (16 nm) bilayer. As shown in figures 5(a) and
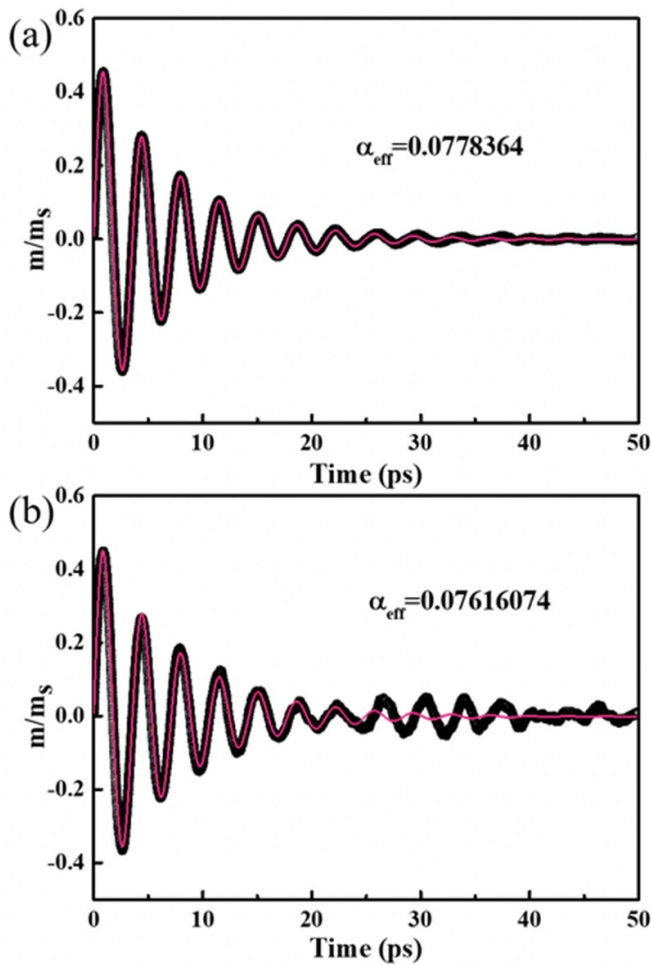
Figure 5. The time evolution of the magnetisation trace (circles) for Py (6 nm)/Nd (16 nm) bilayer. (a) and (b) are low (20 K) and high temperature (500 K) at same integrator-random-seed = 5, respectively. The lines are fitting by equation (16).

(b), (for the same random seed), the magnetisation precession response differs at different temperatures. At low temperature (20 K), as shown in figure 5(a), the influence of the temperature on the simulation is very small and the fitting curve is consistent for the whole time series. However, at high temperature (500 K), as shown in figure 5(b), the thermal-spin fluctuation plays a role on relaxation time. While the fitted damping is very similar in both cases, at the higher temperatures the dynamics at longer times becomes driven by the response of the system to the random thermal fields.

4. Conclusions

In summary, we have investigated the thickness and temperature dependence of the effective magnetic damping in Py (6 nm)/Nd (t nm) bilayer by using the spin accumulation model in an atomistic simulation. The approach used was to simulate the precession to equilibrium after rotation through a small angle. The calculation used an atomistic model to calculate the spin pumping into the non-magnetic capping layer. For large Nd layer thickness, the (supercritical) damping, when associated with a single Py atomic layer, was found to give rise to discrepancies with experiment and it was found necessary to spread the elevated damping of two Py layers. This problem and its solution is an interesting prediction of the atomistic model and probably arises from interface diffusion. Therefore, the calculations were carried out on a system of Py (bulk)/Py (2-monolayer)/Nd (*t*) layers. Through a series of calculations, we determined the damping value of the bulk-Py and the 2-monolayer-Py, with the Nd as a non-magnetic material. The thickness dependence of the effective magnetic damping value from the simulations is consistent with the experimental data. Further, the effect of temperature on the mean magnetic damping was also carefully investigated. With increasing temperature, the influence of thermal fluctuations on mean magnetic damping increases, which is probably a finite size effect. Our results show that the combination of atomistic and spin accumulation models is a powerful approach to the investigation of spin pumping in heterostructures, especially where interfacial mixing is likely.

Data availability statement

All data that support the findings of this study are included within the article (and any supplementary files).

Author contributions

Lulu Cao performed the sample preparation, measurements, atomistic simulations, analysed the data and drafted the manuscript; Sergiu Ruta, Richard F L Evans, Phanwadee Chureemart and Roy W Chantrell performed atomistic and spin accumulation calculations, analysed the data; Richard F L Evans and Roy W Chantrell modified the manuscript; Richard F L Evans, Roy W Chantrell and Ya Zhai preformed project administration and supervision.

Conflict of interest

The authors declare that they have no known competing financial interests or personal relationships that could have appeared to influence the work reported in this paper.

ORCID iDs

Lulu Cao ⓘ https://orcid.org/0009-0005-7572-5780
Sergiu Ruta ⓘ https://orcid.org/0000-0001-8665-6817
Rungtawan Khamtawi ⓘ https://orcid.org/0009-0008-9057-2948
Phanwadee Chureemart ⓘ https://orcid.org/0000-0002-1199-7809
Ya Zhai ⓘ https://orcid.org/0000-0002-9006-9575
Richard F L Evans ⓘ https://orcid.org/0000-0002-2378-8203
Roy W Chantrell ⓘ https://orcid.org/0000-0001-5410-5615

References

[1] Gallagher W J and Parkin S S P 2006 Development of the magnetic tunnel junction MRAM at IBM: from first junctions to a 16-Mb MRAM demonstrator chip *IBM J. Res. Dev.* **50** 5

[2] Chen Q, Ruan X, Yuan H, Zhou X, Kou Z, Huang Z, Xu Y and Zhai Y 2020 Interlayer transmission of magnons in dynamic spin valve structures *Appl. Phys. Lett.* **116** 132403

[3] Zhang W, Zhang D, Wong P K J, Yuan H, Jiang S, van der Laan G, Zhai Y and Lu Z 2015 Selective tuning of Gilbert damping in spin-valve trilayer by insertion of rareearth nanolayers *ACS Appl. Mater. Interfaces* **7** 17070

[4] Gajek M *et al* 2012 Spin torque switching of 20 nm magnetic tunnel junctions with perpendicular anisotropy *Appl. Phys. Lett.* **100** 132408

[5] Rebei A and Hohlfeld J 2006 Origin of increase of damping in transition metals with rare-earth-metal impurities *Phys. Rev. Lett.* **97** 117601

[6] Luo C *et al* 2014 Enhancement of magnetization damping coefficient of permalloy thin films with dilute nd dopants *Phys. Rev. B* **89** 184412

[7] Yue J, Jiang S, Zhang D, Yuan H, Wang Y, Lin L, Zhai Y, Du J and Zhai H 2016 The influence of interface on spin pumping effect in $Ni_{80}Fe_{20}$/Tb bilayer *AIP Adv.* **6** 056120

[8] Luo C, Zhang W, Wong P K J, Zhai Y, You B, Du J and Zhai H 2014 The influence of Nd dopants on spin and orbital moments in Nd-doped permalloy thin films *Appl. Phys. Lett.* **105** 082405

[9] Tserkovnyak Y, Brataas A and Bauer G E W 2002 Enhanced Gilbert damping in thin ferromagnetic films *Phys. Rev. Lett.* **88** 117601

[10] Tserkovnyak Y, Brataas A and Bauer G E W 2002 Spin pumping and magnetization dynamics in metallic multilayers *Phys. Rev. B* **66** 224403

[11] Zhang S, Levy P M and Fert A 2002 Mechanisms of spinpolarized current-driven magnetization switching *Phys. Rev. Lett.* **88** 236601

[12] Barati E and Cinal M 2015 Quantum mechanism of nonlocal gilbert damping in magnetic trilayers *Phys. Rev. B* **91** 214435

[13] Liu Y, Yuan Z, Wesselink R, Starikov A A and Kelly P J 2014 Interface enhancement of Gilbert damping from first principles *Phys. Rev. Lett.* **113** 207202

[14] Zhao Y, Song Q, Yang S H, Su T, Yuan W, Parkin S S P, Shi J and Han W 2016 Experimental investigation of temperature-dependent Gilbert damping in permalloy thin films *Sci. Rep.* **6** 22890

[15] Foros J, Woltersdorf G, Heinrich B and Brataas A 2005 Scattering of spin current injected in Pd(001) *J. Appl. Phys.* **97** 10A714

[16] Evans R F L, Fan W J, Chureemart P, Ostler T A, Ellis M O A and Chantrell R W 2014 Atomistic spin model simulations of magnetic nanomaterials *J. Phys.: Condens. Matter* **26** 103202

[17] 2020 VAMPIRE software package v5 available from (available at: https://vampire.york.ac.uk/)

[18] Aronov A 1976 Spin injection in metals and polarization of nuclei *JETP Lett.* **24** 37–39

[19] Chureemart P, D'Amico I and Chantrell R W 2015 Model of spin accumulation and spin torque in spatially varying magnetisation structures: limitations of the micromagnetic approach *J. Phys.* **27** 146004

[20] Jedema F J, Filip A T and van Wees B J 2001 Electrical spin injection and accumulation at room temperature in an all-metal mesoscopic spin valve *Nature* **410** 345

[21] Heide C, Zilberman P E and Elliott R J 2001 Currentdriven switching of magnetic layers *Phys. Rev. B* **63** 064424

[22] Sampan-a-pai S, Chureemart J, Chantrell R W, Chepulskyy R, Wang S, Apalkov D, Evans R F L and Chureemart P 2019 Temperature and thickness dependence of statistical fluctuations of the Gilbert damping in bilayers *Phys. Rev. Appl.* **11** 044001

[23] Callen H and Callen E 1966 The present status of the temperature dependence of magnetocrystalline anisotropy, and the $l(l + 1)/2$ power law *J. Phys. Chem. Solids* **27** 1271

[24] Zener C 1954 Classical theory of the temperature dependence of magnetic anisotropy energy *Phys. Rev.* **96** 1335

[25] Moon R M, Cable J W and Koehler W C 1964 Magnetic structure of neodymium *J. Appl. Phys.* **35** 1041

[26] Irkhin Y P 1988 Electron structure of the 4f shells and magnetism of rare-earth metals *Sov. Phys. - Usp.* **31** 163

[27] Mizukami S, Ando Y and Miyazaki T 2001 Ferromagnetic resonance linewidth for NM/80NiFe/NM films (NM=Cu, Ta, Pd and Pt) *J. Magn. Magn. Mater.* **226–230** 1640